



## A GEOMETRICAL SURFACE TEXTURE STUDY OF SLIDING SLEEVES AND PINS AFTER BENCH TESTS

Krzysztof OLEJARCZYK , Marcin WIKŁO \* 

Casimir Pulaski Radom University, Radom, Poland

\* Corresponding author, e-mail: [m.wiklo@uthrad.pl](mailto:m.wiklo@uthrad.pl)

### Abstract

Objectives was to determine the durability of pins and sleeves used in the construction of a cycloidal gear. The methods used were based on a comparative analysis of selected macro photos of their surfaces and representative surface profiles recorded before and after the bench tests and the Ra and Rz surface roughness values determined on their basis. Before and after the bench tests, the weight of each sleeve and pin was measured, their surface profiles were recorded and micro photos of these surfaces were taken. Based on each recorded surface profile, the roughness parameters Ra and Rz were determined. The advantages of using steel sleeves in the cycloidal drive structure, increasing its durability, have been demonstrated by the low mass wear of the sleeves and the low surface roughness parameters Ra and Rz. It was shown that the appropriate accuracy of the pins and sleeves is necessary.

Keywords: cycloidal drive, geometrical surface texture, sleeves, pins

### 1. INTRODUCTION

The main problems in the field of maintenance are ensuring high reliability and readiness to start work [1]. High requirements as to durability and reliability make it necessary to obtain information about the condition of devices during maintenance [2].

Due to the use of a cycloidal drive at structures with high loads, its individual components must be highly resistant to wear to ensure the long life of the gear. The structure of the tested cycloidal drive is shown in Fig. 1.

The sliding sleeves and pins are made of the same material as cycloidal discs: 32CDV13 steel. Sliding sleeves, pins and cycloidal discs have undergone the same heat treatment for which the hardness of the 44HRC elements was achieved. The outer surfaces of each sliding sleeve and pin were ground. The article [3] presents the research on the impact of slide burnishing process carried out with use of various ceramics on friction and wear of steel elements. In addition, surfaces after grinding, lapping and polishing processes were tested

The sliding burnishing process enables to obtain an increased hardness in the surface layer [4, 5] and to obtain a very good surface smoothness [6]. These features favorably affect a number of functional properties, including tribological wear [7] and fatigue strength [5, 8].

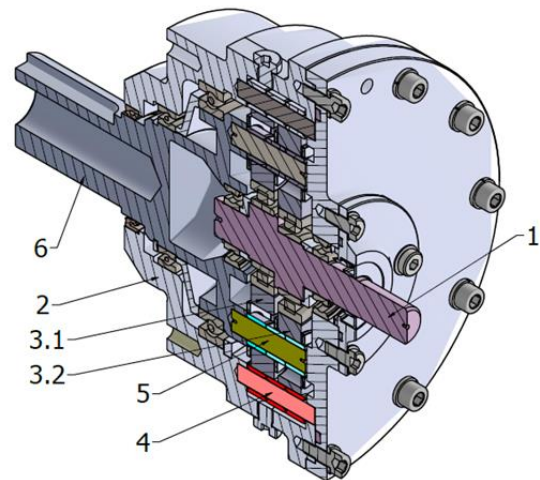


Fig. 1. Cross-section of the cycloidal drive:  
1 – input shaft, 2 – housing,  
3.1, 3.2 – cycloidal discs, 4 – outer pins with sliding sleeves, 5 – inner pins with sliding sleeves,  
6 – output shaft

The research results concerning the influence of variables loads on the maintenance characteristics of sliding bearings have been published [9]. The issues related to geometrical surface texture were investigated in [10–12]. The publications [13, 14] present the methodology of designing a cycloidal drive and describe the influence of selected

geometrical parameters on its durability. Kinematic error analysis and tolerance allocation of cycloidal drive reducers were investigated [15]. Tooth modification and dynamic performance [16]. [17] presents the results of cycloidal drive tests in terms of the application of slide and needle roller bearings. The primary issues of cycloidal discs durability in experimental studies were investigated in [18]. The tests results of sliding sleeves mounted on internal pins, made of bronze and used in cycloidal drive, are presented in [19]. Their very high sensitivity to wear was the reason for undertaking further research on reducing the wear effect. The article [20] considered planetary gear vibration response to detect gear pitting due to wear. The research objects assumed in this article are all external and internal pins and the sleeves installed on them. Such a comprehensive approach to the study of these kinematic pairs allowed for a better analysis of the obtained results and drew the correct conclusions.

## 2. ASSUMPTIONS OF THE BENCH TESTS

Based on the analysis of the forces acting on the slide sleeves [13], a decision was made to use steel slide sleeves, replacing the previously used SELFOIL® bronze sleeves made in the powder sintering process. Each sliding sleeve and pin were marked at the production stage with their own

individual number, which made it easier to identify the cooperating surfaces of individual components at the experimental and measuring stage.

A METTLER AT261 laboratory balance was used to measure the weight of the sleeves and pins. The Taylor Hobson Form Talysurf PGI 830 profilograph was used to measure the surface roughness of the tested elements, record the wear pattern profile and surface topography. Profilograph Form Talysurf PGI 830 from Taylor Hobson is a measuring system for roughness, waviness, and shape determination, using the contact method. The measurement is carried out using a sensor with a PGI 830 laser head, which moves along the tested surface. The surface condition was analysed with the use of a Nikon MM 40 / L3FA optical microscope. This type of microscope, together with the MultiScanBase digital image acquisition and processing system, is used to observe the surface of test elements and to observe traces of wear.

Operating parameters of the cycloidal drive during the bench test: temperature of the working environment temperature  $t = 25^{\circ}\text{C}$ , input rotational speed  $n_w = 3500\text{rpm}$ , load  $T = 32\text{Nm}$ , The number of measuring cycles was set to 50 while the time of a single cycle was 1h [21].

The test bench illustrated in Fig. 2 enables testing with different braking torques and input rotational velocities.

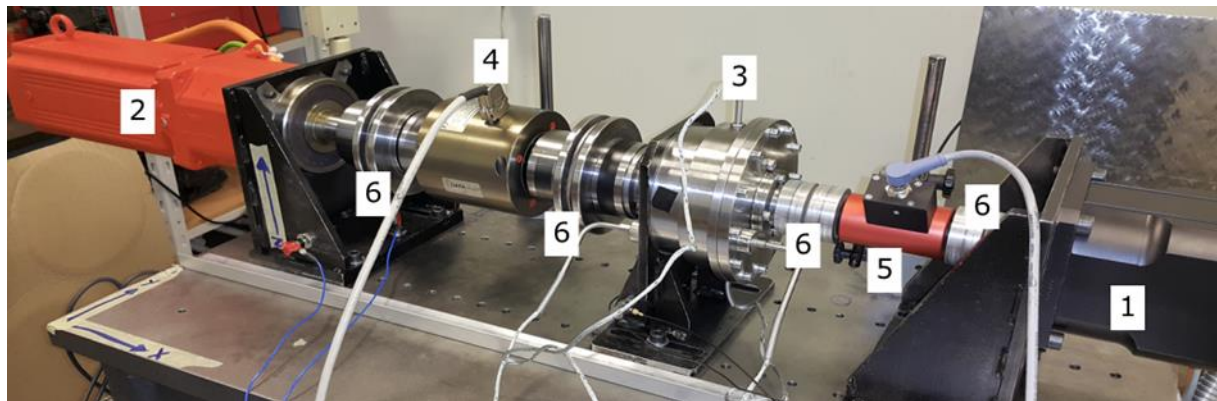


Fig. 2. Test bench: 1-input engine, 2-braking torque, 3-reducer, 4-output torque measurement (collecting data: output velocity, output torque), 5-input torque measurement (collecting data: input velocity, input torque), 6-elastic clutches

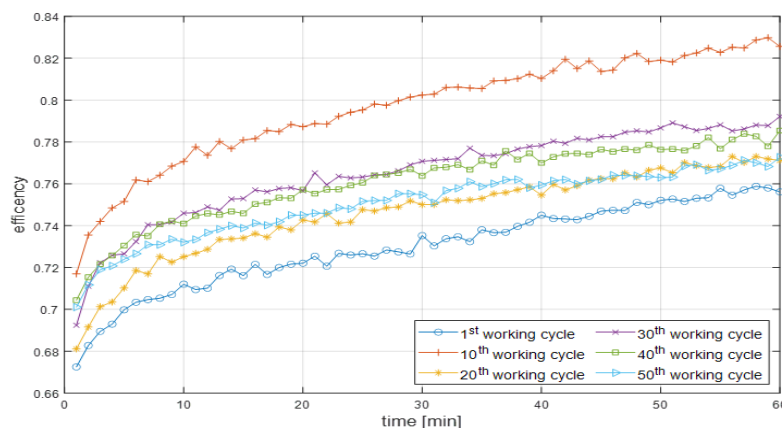


Fig. 3. Summary of cycloidal drive efficiency values calculated for the selected measuring cycles

The efficiency was controlled during the tests according to the procedure presented in [22] where the theoretical and experimental values were verified. The results every 10 cycles are presented in the Fig. 3. An increase in the efficiency in time can be observed, regardless of the measuring cycle, which is conditioned by the oil temperature increase in the cycloidal gear. It can be noted that in the increase of the working cycles the efficiency curves are getting closer to each other which means that the gearbox is already ran-in and the inspection of the wear of the components can be performed.

A comparison of the recorded performance efficiency characteristics of the cycloidal gearbox working with steel sliding sleeves and with sliding bearings made of sintered bronze and presented in [22] shows a significant similarity. Based on this, it can be concluded that a change in the material used for the sliding sleeves in a cycloidal drive does not result in almost any loss change.

### 3. MASS WEAR

To determine the mass wear of the inner and outer sleeves, the mass of each element was measured before and after the bench tests. The average mass of the selves at the beginning of the trial was 8.8143 grams. Fig. 4 and Fig. 5 present

respectively the calculated mass difference of the inner and outer sleeves

On the inner and outer pins, there were two sleeves, which is why in pictures 3 and 4 there is twice higher number of sleeves. The first set for inner (1-8) and external (1-16) pins was working with the cycloidal gear wheel depicted in the Fig. 2 pos. 3.1 and the second set of sleeves for inner (9-16) and external (17-32) with pos. 3.2. An analysis of the mass wear of the inner sleeves and outer sleeves shows maximal weight loss at value  $1.94 \cdot 10^{-3}$  g and  $1.6 \cdot 10^{-3}$  g which nevertheless is not equal for each pin which can be caused by the manufacturing and assembly tolerance.

### 4. THE CONDITION OF THE SURFACE OF THE INNER PINS AND OUTER PINS AND THE STEEL SLIDING SLEEVES MOUNTED ON THEM

To determine the visual state of the surfaces of the selected pins and sleeves, macro photos were taken at 100 times magnification. Fig. 5 shows exemplary photographs of the condition of selected surfaces of pins at the test beginning and after 50 measurement cycles

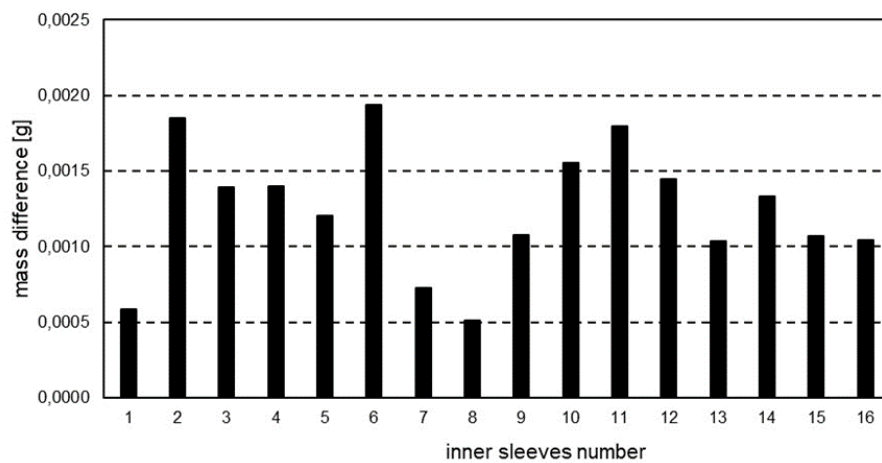


Fig. 4. Measurement results in the form of the mass difference of the inner sleeves

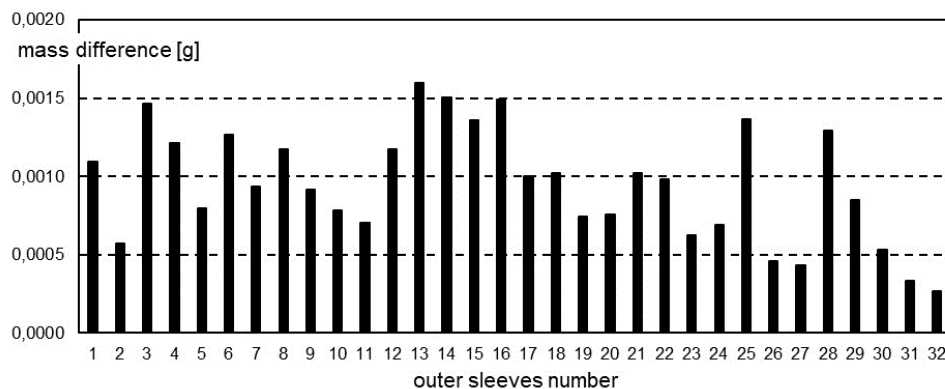


Fig. 5. Measurement results in the form of the mass difference of the outer sleeves

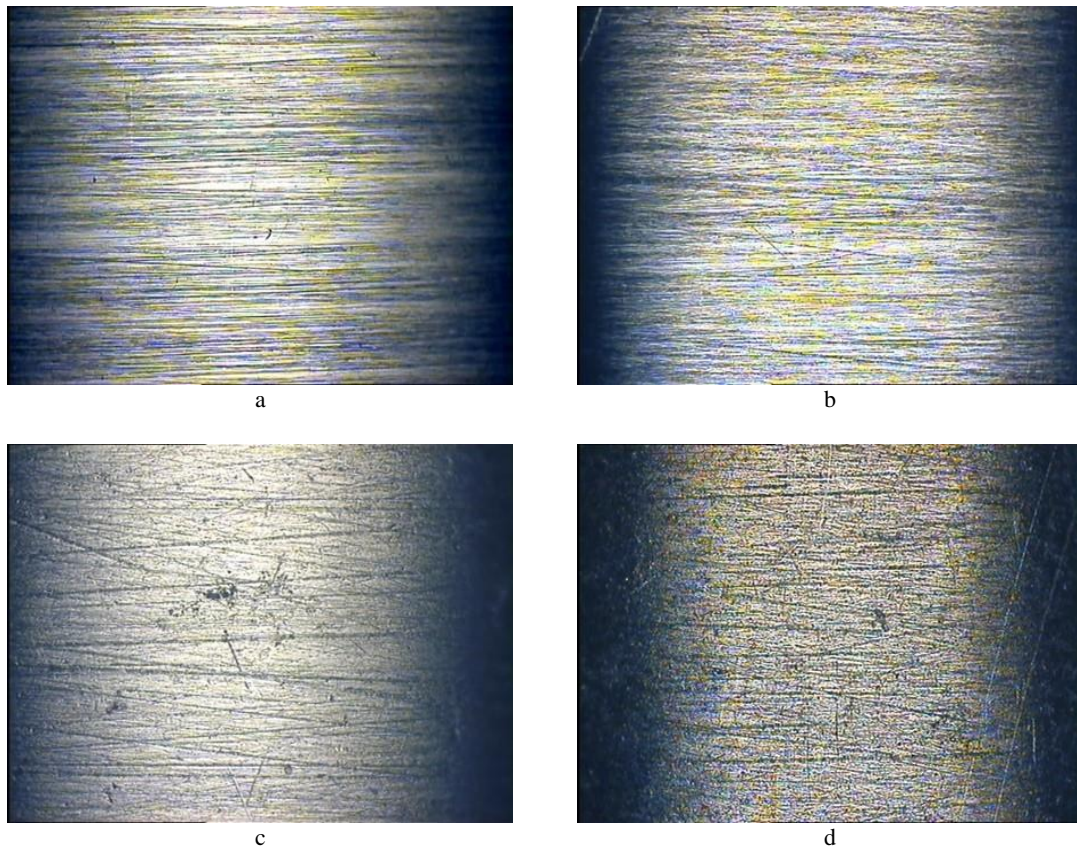


Fig. 1. A list of photographs showing the selected a) new surface of the inner pin no. 4, b) the surface of the inner pin no. 4 after 50 cycles, c) the new surface of the outer pin no. 13, d) the surface of the outer pin no. 13 after 50 cycles

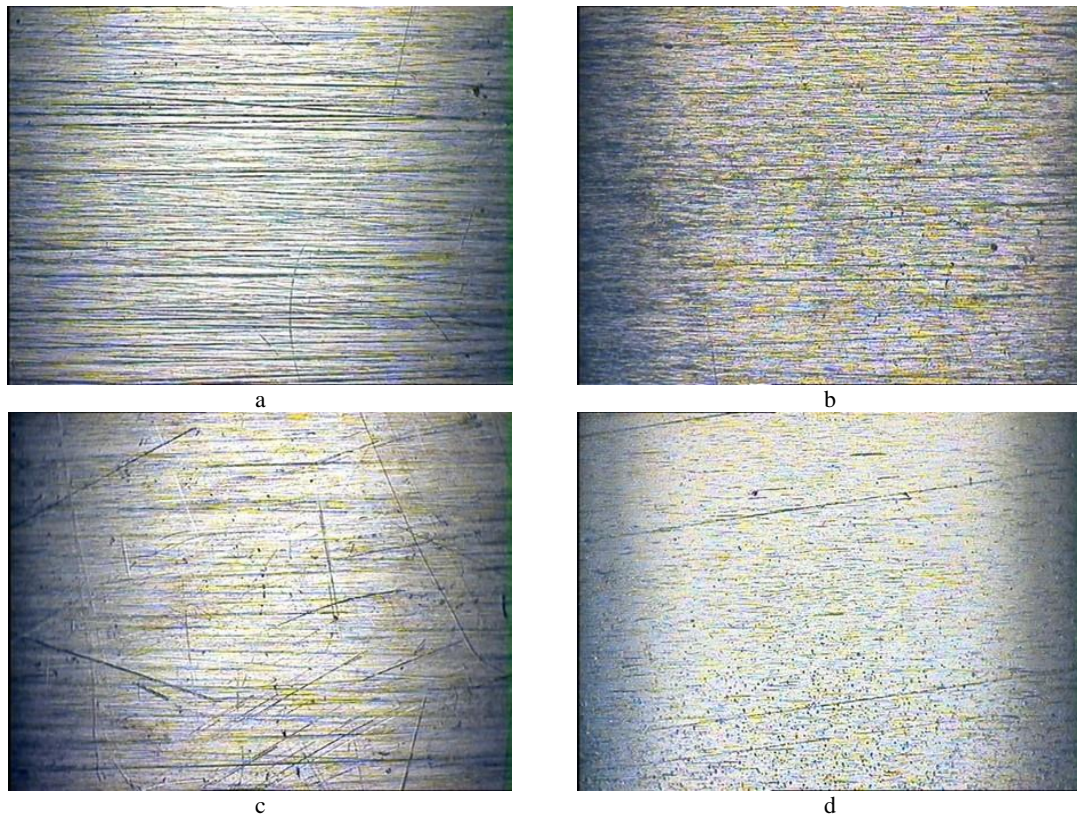


Fig. 7. A list of photographs showing the selected a) new surface of the inner sleeve no. 4, b) surface of the inner sleeve no. 4 after 50 cycles, c) new surface of the outer sleeve no. 3, d) surface of the outer sleeve no. 3 after 50 cycles

Fig. 6 shows examples of photographs of selected surfaces of the new sleeves and after 50 measuring cycles. The photos were taken at 100 times magnification using an optical microscope

The condition of the surfaces shown in Fig. 5 and Fig.6 indicates that they have been lapped. The analysis of the list presented in Fig. 4 allows finding no noticeable effects of pitting wear that occurred after conducting bench tests with the use of SELFOIL® bronze sliding sleeves [21], Fig. 7. Based on the photographic analysis of the surface condition, steel sliding sleeves can be indicated as elements that better transfer loads.

## 5. COMPARATIVE ANALYSIS OF SURFACE PROFILES AND SURFACE ROUGHNESS VALUES

The analyzed gear design has 32 slide sleeves mounted on 16 external pins and 16 slide sleeves mounted on 8 internal pins (Fig. 1).

It was assumed that the profiles of the sleeves and pins were recorded by three longitudinal profiles in the following positions (Fig. 7):

- $0^\circ$  (the surfaces above the number representing the sleeve or pin were selected as a reference point),
- $120^\circ$ ,
- $240^\circ$ .

The left side of the element corresponds to the numbered side of the element.

Figure 7 shows an example of an inner sleeve no.2 for recorded a profile set for an angle of  $0^\circ$ .

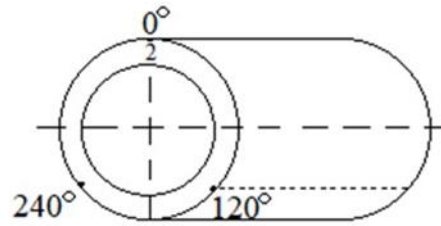


Fig. 8. The assumed system of the measurement profiles on the example of the inner sleeve no.2

The profiles of the new surface of the outer pin no. 4 for the settings  $0^\circ$ ,  $120^\circ$  and  $240^\circ$  are shown in Fig. 8.

The analyzes of all recorded profiles of pins and sliding sleeves indicate quite large discrepancies in shape. This may have an adverse effect on the nature of work in the contact zones of individual kinematic pairs of pin-sleeve, sleeve-cycloidal disc.

Representative profiles of selected surfaces and the results of surface roughness measurements for the inner pin no.1 are shown in Fig. 9.

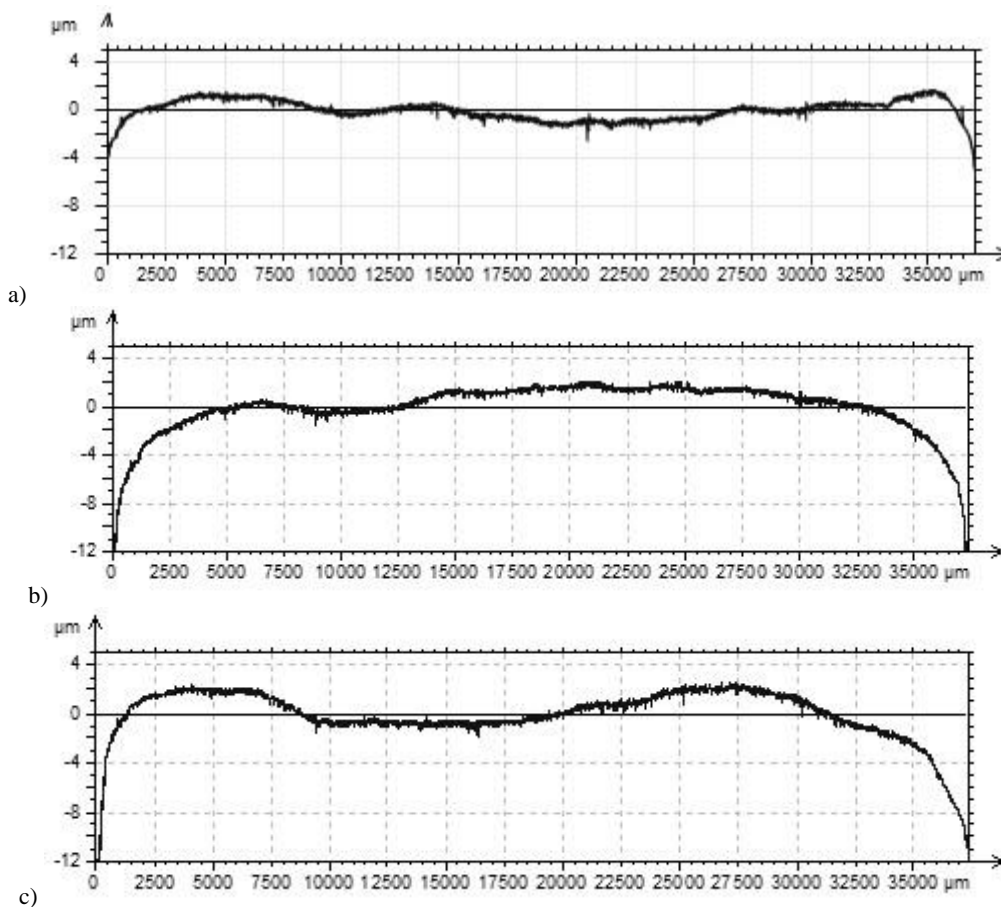


Fig. 9 Profiles of the surface of the outer pin No. 4 for the setting corresponding to the angular value: a)  $0^\circ$ , b)  $120^\circ$ , c)  $240^\circ$

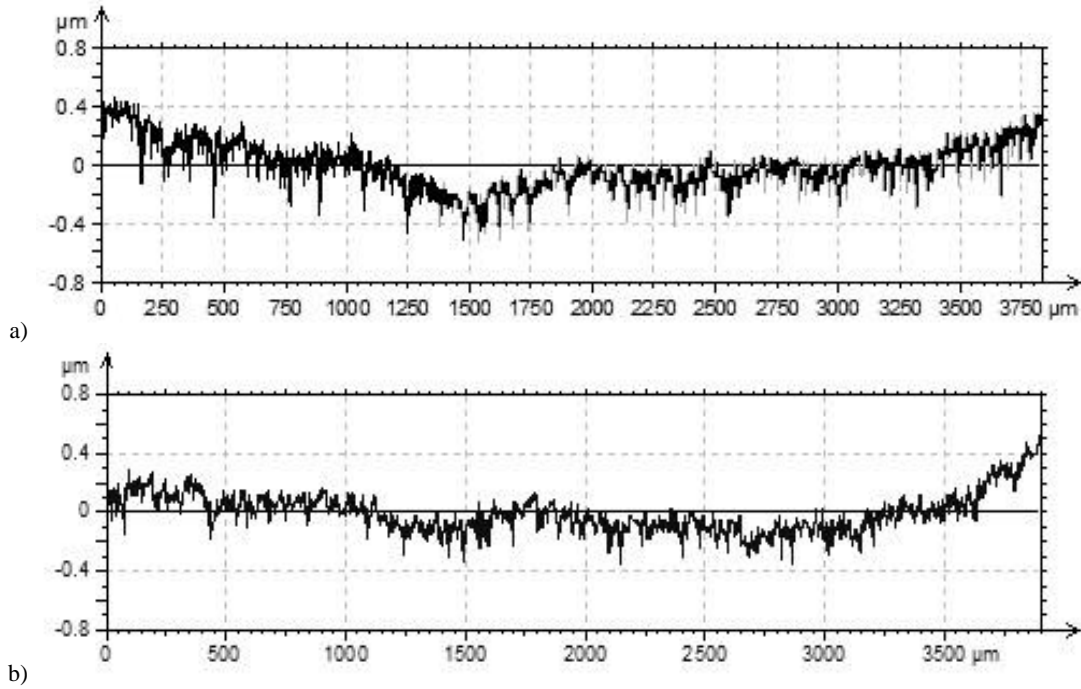


Fig. 10. Profile of the surface of the inner pin no.1 for the setting corresponding to the angular value  $0^\circ$ :  
a) new b) after 50 measuring cycles

The surface roughness values determined on the basis of the registered profile are:

- for the new surface:  $R_a=0.062 \mu\text{m}$ ;  $R_z=0.551 \mu\text{m}$ ;

- for surfaces after 50 cycles:  $R_a=0.053 \mu\text{m}$ ;  $R_z=0.407 \mu\text{m}$ .

Representative surface profiles and the results of surface roughness measurements for the inner sleeve no. 1 are shown in Fig. 10.

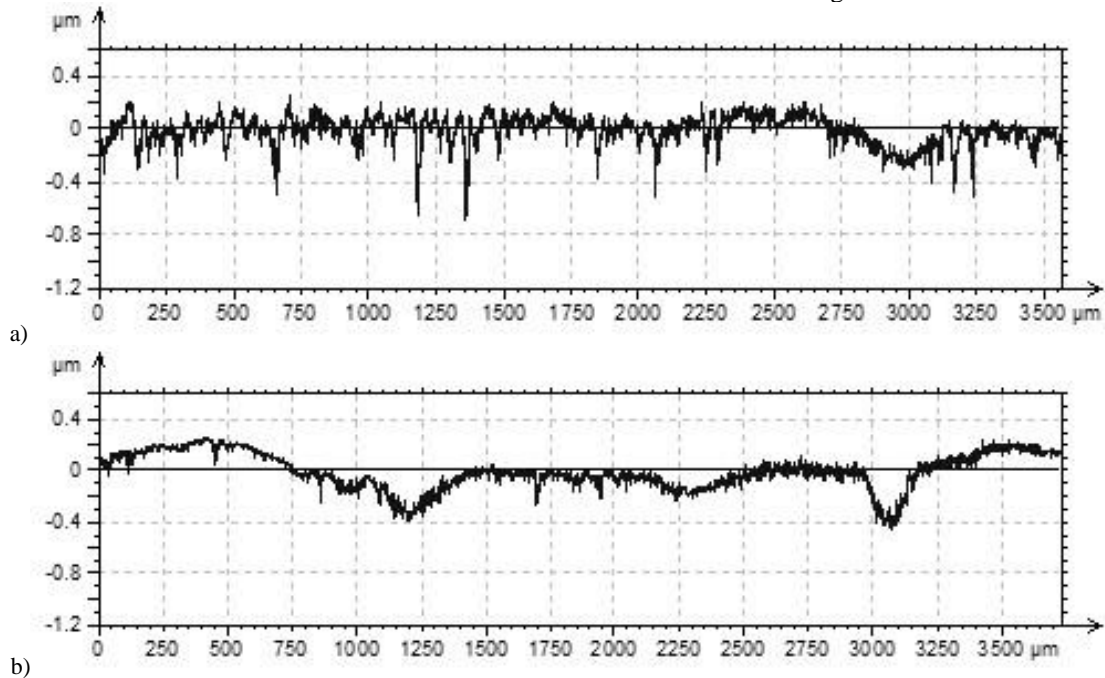


Fig. 11. Surface profile of the inner sleeve no.1 for the setting corresponding to the angular value of  $240^\circ$ :  
a) new b) after 50 cycles

The surface roughness values determined based on the registered profile are:

- for the new surface:  $R_a=0.072 \mu\text{m}$ ;  $R_z=0.709 \mu\text{m}$ ;  
- for surfaces after 50 cycles:  $R_a=0.047 \mu\text{m}$ ;  $R_z=0.340 \mu\text{m}$ .

Representative surface profiles and the results of surface roughness measurements for the outer pin no. 1 are shown in Fig. 11.

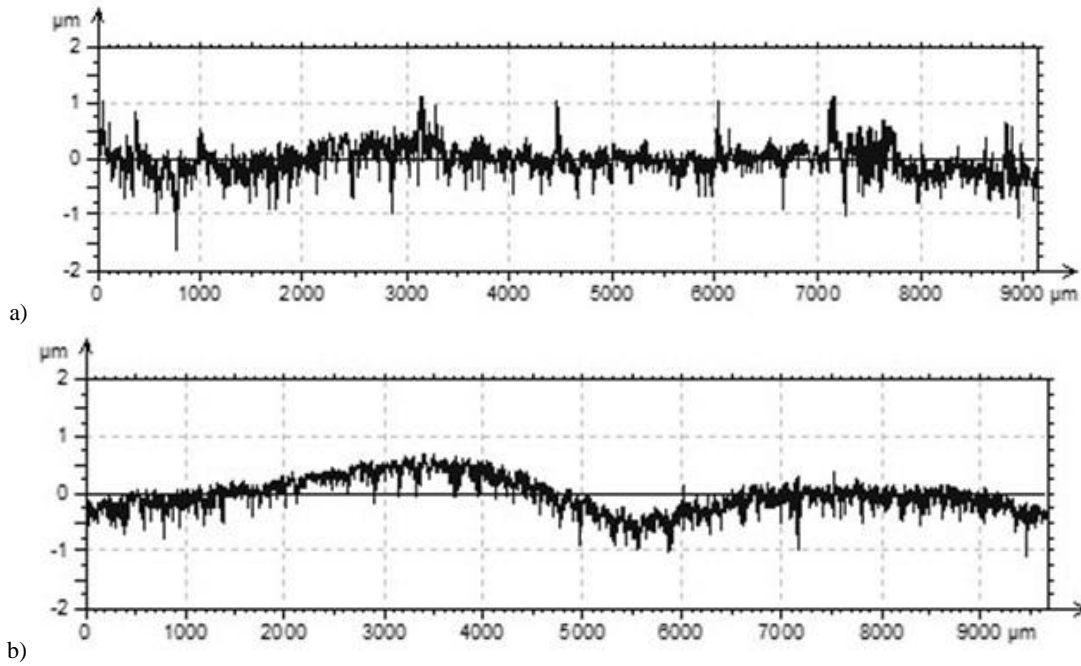


Fig. 12. Surface profile of the outer pin no.1 for the setting corresponding to the angular value of 120°:  
 a) new b) after 50 measuring cycles

The surface roughness values determined based on the registered profile are:  
 - for the new surface:  $R_a=0.161 \mu\text{m}$ ;  $R_z=1.547 \mu\text{m}$ ;

- for surfaces after 50 cycles:  $R_a=0.098 \mu\text{m}$ ;  $R_z=0.858 \mu\text{m}$ .

Representative surface profiles and the results of surface roughness measurements for the outer sleeve no.17 are shown in Fig. 12

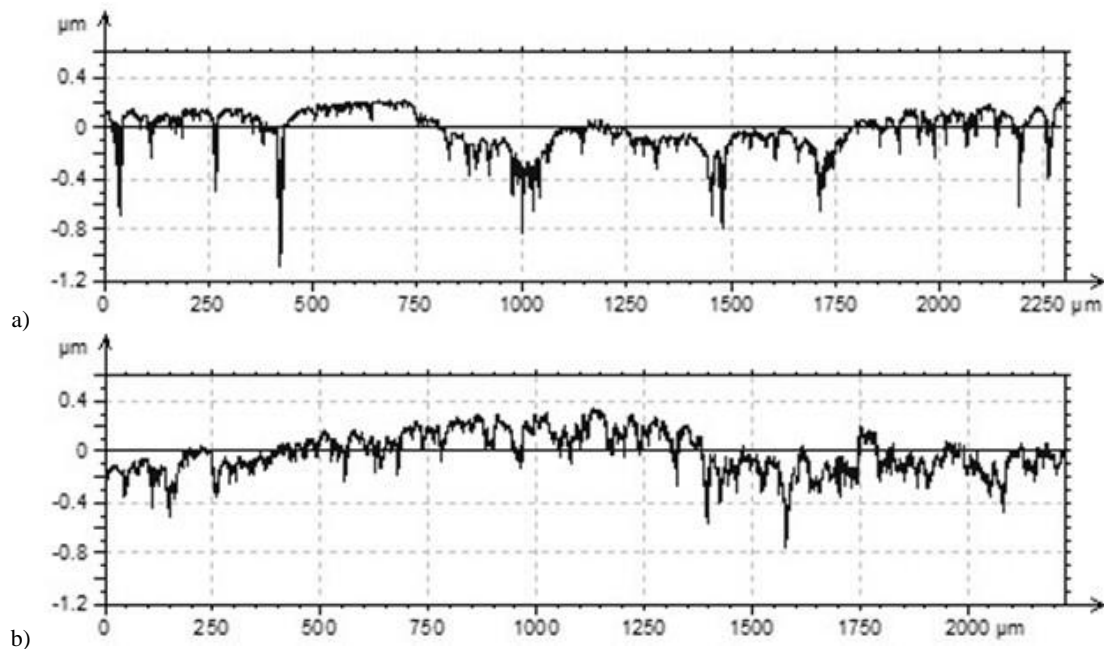


Fig. 13 Surface profile of the outer pin no.17 for the setting corresponding to the angular value 0°:  
 a) new b) after 50 measuring cycles

The surface roughness values determined based on the registered profile are:  
 - for the new surface:  $R_a=0.144 \mu\text{m}$ ;  $R_z=1.087 \mu\text{m}$ ;

- for surfaces after 50 cycles:  $R_a=0.079 \mu\text{m}$ ;  $R_z=0.688 \mu\text{m}$ .

## 6. CONCLUSIONS

1. Mass wear of sleeves after 50 measuring cycles is in range 1.6e-3g to 1.84g and is equal to it can also be noted that the mass wear is not equal for all the sleeves.
2. Record profiles of new surfaces of the sleeves and pins indicate manufacturing errors. Therefore, it seems necessary to ensure the control of the execution of these transmission elements.
3. The analysis of the roughness values Ra and Rz determined from the recorded surface profiles showed their reduction after 50 measuring cycles.
4. The analysis of wear traces using macro photos, recorded surface profiles and a comparative analysis of the determined Ra and Rz roughness values on the surfaces of pins and sliding sleeves after 50 measuring cycles indicates the need to extend the time interval of the tests to observe greater wear effects.

**Author contributions:** *research concept and design, K.O., M.W.; Collection and/or assembly of data, K.O.; Data analysis and interpretation, M.W.; Writing the article, K.O.; Critical revision of the article, M.W.; Final approval of the article, K.O., M.W.*

**Declaration of competing interest:** *The authors declare that they have no known competing financial interests or personal relationships that could have appeared to influence the work reported in this paper.*

## REFERENCES

1. Drożdź P. The influence of the vehicle work organization conditions on the engine start-up parameters. *Eksploatacja i Niezawodność - Maintenance and Reliability* 2008; 37: 72–4.
2. Batko W, Borkowski B, Głocki K. Application of database systems in machine diagnostic monitoring. *Eksploatacja i Niezawodność*. 2008;1: 7–10.
3. Dzierwa A, Gałda L, Tupaj M, Dudek K. Investigation of wear resistance of selected materials after slide burnishing process. *Eksploatacja i Niezawodność – Maintenance and Reliability* 2020; 22(3): 432–9. <https://doi.org/10.17531/ein.2020.3.5>.
4. Saldaña-Robles A, Plascencia-Mora H, Aguilera-Gomez E, Saldaña Robles A, Márquez-Herrera A, Diosdado De la Peña JA. Influence of ball-burnishing on roughness, hardness and corrosion resistance of AISI 1045 steel. *Surface and Coatings Technology* 2018; 339 <https://doi.org/10.1016/j.surfcoat.2018.02.013>.
5. Travieso-Rodríguez JA, Jerez-Mesa R, Gómez-Gras G, Llumà-Fuentes J, Casadesús-Farràs O, Madueño-Guerrero M. Hardening effect and fatigue behavior enhancement through ball burnishing on AISI 1038. *Journal of Materials Research and Technology* 2019; 1; 8(6): 5639–5646.
6. Revankar G, Shetty R, Rao S, Gaitonde V. Analysis of surface roughness and hardness in ball burnishing of titanium alloy. *Measurement* 2014; 58 <https://doi.org/10.1016/j.measurement.2014.08.043>
7. Rao DS, Hebbar HS, Komaraiah M, Kempaiah UN. Investigations on the Effect of Ball Burnishing Parameters on Surface Hardness and Wear Resistance of HSLA Dual-Phase Steels. *Materials and Manufacturing Processes* 2008; 23(3): 295–302. <https://doi.org/10.1080/10426910801937306>.
8. Valiorgue F, Zmely V, Dumas M, Chomienne V, Verdu C, Lefebvre F, et.al. Influence of residual stress profile and surface microstructure on fatigue life of a 15-5PH. *Procedia Engineering* 2018; 213: 623–9. <https://doi.org/10.1016/j.proeng.2018.02.058>.
9. Ponieważ G, Kuśmierz L. Numerical research of the influence of loading and edge support element of self aligning pad on contact zone properties. *Eksploatacja i Niezawodność - Maintenance and Reliability* 2007; 10–14. <https://archive.ein.org.pl/2007-02-02>.
10. Mainsah E, Greenwood JA, Chetwynd DG, editors. *Metrology and Properties of Engineering Surfaces*. Boston, MA: Springer US 2001.
11. Nowicki B. *Struktura geometryczna. Chropowatość i falistość powierzchni*. Warszawa: WNT 1991.
12. Wos S, Koszela W, Dzierwa A, Reizer R, Pawlus P. Effects of oil pocket shape and density on friction in reciprocating sliding. *Eksploatacja i Niezawodność – Maintenance and Reliability* 2022; 24(2): 338–45. <https://doi.org/10.17531/ein.2022.2.15>.
13. Chmurawa M. Cycloidal gears with tooth modification. *Silesian Technical University, Zeszyty naukowe*, Nr 1547; 2002.
14. Bednarczyk S. Rozwój obiegowych przekładni cykloidalnych ukierunkowany na podniesienie efektywności maszyn. *Efektywność wykorzystania maszyn roboczych i urządzeń w przemyśle*. Idzikowski, A. Częstochowa: WZ Politechnika Częstochowska 2013; 117–125.
15. Lin KS, Chan KY, Lee JJ. Kinematic error analysis and tolerance allocation of cycloidal gear reducers. *Mechanism and Machine Theory* 2018; 124: 73–91. <https://doi.org/10.1016/j.mechmachtheory.2017.12.028>.
16. Olejarczyk K, Wikło M, Kołodziejczyk K, Król K, Nowak R. Experimental impact studies of the application mineral oil and synthetic oil on the efficiency of the single-gear cycloidal. *Tribologia* 2017; 1: 67–73.
17. Olejarczyk K, Kalbarczyk M. A Geometrical surface texture study of cycloid drive discs after bench tests. *Tribologia* 2021; 297(3): 27–33. <https://t.tribologia.eu/gicid/01.3001.0015.6894>
18. Warda B. Stanowisko do badania trwałości zazębienia obiegowej przekładni cykloidalnej. *Tribologia* 2006; 6: 131–140.
19. Żurowski W, Olejarczyk K, Zaręba R. Wear Assessment of Sliding Sleeves in a Single-Stage Cycloidal Drive. *Advances in Science and Technology*. *Research Journal* 2019; 13(4): 239–245. <https://doi.org/10.12913/22998624/114180>.
20. Berlato F, D’Elia G, Battarra M, Dalpiaz G. Condition monitoring indicators for pitting detection in planetary gear units. *Diagnostyka* 2020; 21(1): 3–10. <https://doi.org/10.29354/diag/116079>.
21. Dubaish AA, Jaber AA. Fabrication of a test rig for gearbox fault simulation and diagnosis. *Diagnostyka* 2023; 24(2): 1–8. <https://doi.org/10.29354/diag/162541>.
22. Olejarczyk K, Wikło M, Kołodziejczyk K. The cycloidal gearbox efficiency for different types of bearings—Sleeves vs. needle bearings. *Proceedings of*



the Institution of Mechanical Engineers, Part C:  
Journal of Mechanical Engineering Science 2019;  
233(21–22): 7401–7411.  
<https://doi.org/10.1177/0954406219859903>.



**Dr. Krzysztof  
OLEJARCZYK,**

is a researcher with experience in designing, testing the efficiency and durability of high-ratio gears used in multi-axis manipulators. He specializes in the study of cycloidal drive. His objective is to apply the acquired skills and knowledge for the development

and application of gears in manipulators.

e-mail: [k.olejarczyk@uthrad.pl](mailto:k.olejarczyk@uthrad.pl)



**Marcin WIKŁO, Ph. D.,**

researcher at the Casimir Pulaski Radom University, is the head of the Digital Technology Centre. Experience gained during the implementation of scientific projects and orders carried out for the industry, including designing 6-axis robots and cycloidal gears for the aerospace. Since 2021 associated

with the Future Industry Platform.

e-mail: [m.wiklo@uthrad.pl](mailto:m.wiklo@uthrad.pl)